SIMULATIONS TO FLATTEN THE FIELD OF THE FETS RFQ

S. Lawrie, A. Letchford, ISIS Neutron Source, Rutherford Appleton Laboratory, Oxfordshire, UK.
J. Pozimski, P. Savage, Department of Physics, Imperial College, London, UK.

Abstract

A high performance radio frequency quadrupole (RFQ) is the next major component to be installed at the front end test stand (FETS) at the Rutherford Appleton laboratory (RAL) in the UK. Apart from minor tweaks, the beam dynamics, RF, thermal and mechanical designs of the RFQ are complete. The copper has been purchased and machining is expected to commence in September. This report summarizes the simulation work performed to ensure the RF design is sound. This includes performance studies of the end-wall dipole suppression fingers, tuning the frequency of the input and output vane end regions and implementing a simple solution to remove modulation induced field tilt.

INTRODUCTION

A four-vane RFQ [1] has been designed for the FETS project [2] to accelerate a 60mA H^- ion beam to 3MeV with 95% transmission at up to 10% duty cycle. An RFQ is a 'one-knob' machine with only the input RF power (and hence inter-vane voltage) adjustable. Options are thus limited to correct for any errors in manufacturing that may affect the RF fields inside the cavity and hence beam transmission. This paper details the simulations performed and modifications implemented to anticipate any problems that may occur. The RFQ will be bolted together so further small adjustments will be possible.

BEAM DYNAMICS

The FETS 324MHz RFQ will accelerate a 65keV, 60mA H^- ion beam with a normalised RMS transverse emittance of 0.25 π mm mrad, at pulse lengths of up to 2ms at 50Hz. The beam is generated by an upgraded ISIS Penning ion source and focussed into the RFQ by a three-solenoid magnetic low energy beam transport (LEBT). Letchford's RFQSIM [3] code generated the 308 modulation parameters based on a vane-tip voltage of 42.5kV, or 1.7 times the Kilpatrick field. With the proviso that the vane tip radius, ρ is held fixed at 3.100mm to ease machining, both RFQSIM and particle tracking through field maps [4] predict beam transmission of 95%.

The beam dynamics design requires a constant (or 'flat') vane-tip voltage along the RFQ; whereas some higher energy RFQs have an increasing voltage to prevent the length becoming prohibitive [5]. This being the case, the standard procedure of individually positioning movable slug tuners will be performed to ensure the RFQ has a flat field. Some other laboratories have found [6, 7] that significant movement of the tuners was required to create a flat field; affecting the resonant frequency. Provided the tuners have enough travel range this can be cured, but not without side effects such as lower Q. This being the case, a study was performed of the FETS RFQ to ensure the field is approximately flat and resonates on tune to begin with, thus easing the tuning procedure post-manufacture.

DIPOLE SUPPRESSION FINGERS

For RFQs with vane length l_v comparable to the wavelength λ of the accelerating mode, higher-order mode mixing can occur; the most problematic being the TE110 dipole mode. Methods must be implemented in long RFQs to move the dipole mode away from the desired TE210 quadrupole mode by several MHz. Rather than fixed pi-mode stabilising loops, the FETS RFQ will use adjustable fingers mounted on the end walls [8].

Preliminary tests on the RFQ cold model showed how modifications to the end wall regions affect the resonant frequency and Q [9]. Figs. 1 & 2 show ANSYS simulation results of a 1m RFQ section when varying the position and length of dipole suppression fingers. The fingers allow for great flexibility when tuning the RFQ. Operating at the quadrupole mode, up to 20W of heat will be deposited per finger so the end walls will be cooled.

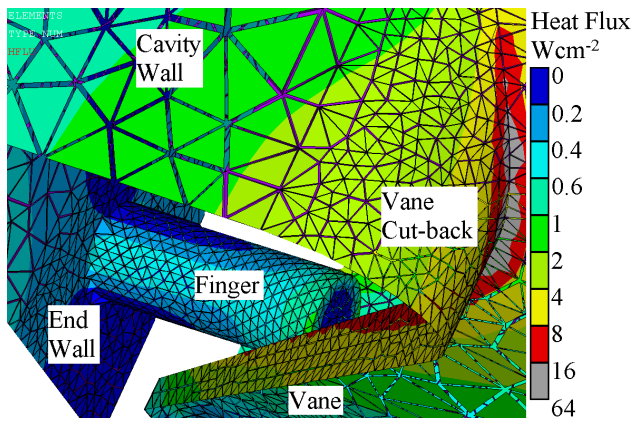

Figure 1: Close-up of RFQ end region showing the heat flux absorbed by a 25mm-long dipole suppression finger.

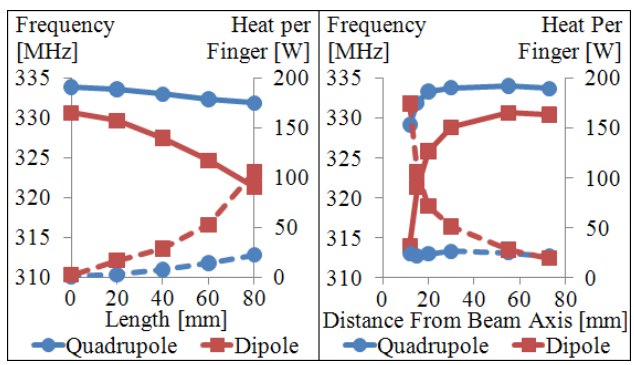

Figure 2: Frequency (solid lines) and heat dissipation (dashed lines) of quadrupole and dipole modes as a function of finger length and transverse position.

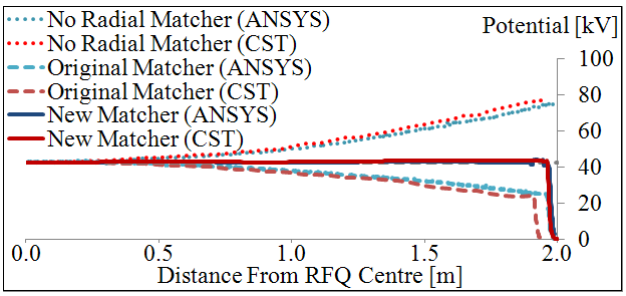

Figure 3: Field tilting effect of an end region with incorrect resonant frequency. The new correctly tuned end region design achieves a field flatness of 3%.

RADIAL MATCHER & VANE CUTBACK

Cavity eigenmode simulations in both CST and ANSYS of the full 4m RFQ showed a non-uniform electric field along the length. As shown in Fig. 3, when the input radial matcher was included on the (unmodulated) vanes, the field was depressed at the ends of the RFQ. With no radial matcher, as in the cold model, the field peaked at the ends. The 40% variance in field amplitude in both cases is thus directly caused by the end regions.

Resonant cavities support an infinite number of modes n, with unperturbed longitudinal field distributions ${}^0V_n(z)$:

$$ {}^0V_n(z) = \sqrt{\frac{2}{l_v}} C_n \quad \text{where: } C_n = \cos\left(\frac{n\pi z}{l_v}\right) \qquad (1) $$

where z is the longitudinal position and l_v is the length of the RFQ vanes [10]. The fundamental $n = 0$ mode has a flat field. Transmission line models of RFQs show how a frequency error $\delta\omega_0$ at some point z_0 causes the modes to mix, creating perturbed fields $\delta V_0(z)/V_0$ given by

$$ \frac{\delta V_0(z)}{V_0} = -8\frac{\delta\omega_0}{\omega_0}\left(\frac{\ell_V}{\lambda}\right)^2 \sum_{n=1}^{\infty} \frac{\cos(n\pi z_0 / l_v)}{n^2} C_n \qquad (2) $$

where $\omega_0 = 2\pi f_0$ is the angular frequency of the fundamental mode (FETS RFQ f_0 = 324MHz). Modes closest to the fundamental contribute most to the perturbation and long RFQs suffer more from this effect.

The negative sign in (2) implies that a region in the RFQ with a high local frequency will force the field down at that position, and vice versa. The reduced/increased field at the ends of the RFQ shown in Fig. 3 is caused by a local frequency increase/reduction when there is/isn't a radial matcher included on the vanes.

Resonant frequency is inversely proportional to the inductance L and capacitance C by

$$ \omega_0 = \frac{1}{\sqrt{LC}} \qquad (3) $$

Alterations to the high magnetic field (inductance) vane cut-backs and the high electric field (capacitance) radial matcher thus allowed the end region to be tuned to the correct frequency using CST Studio. Fig. 4 shows the electric field of the final end region design and Fig. 3 shows the much improved field flatness using this design.

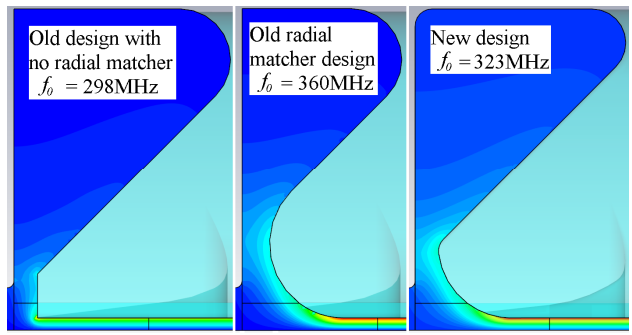

Figure 4: Electric field of RFQ end region, showing geometry changes required to tune for correct frequency.

MODULATION-INDUCED FIELD TILT

Simulating Individual Modulations

The increased depth and length of modulations at the high energy end of long RFQs reduces capacitance. From (3), this results in higher local frequencies and hence, from (2), a reduced field. Simulating the entire RFQ with modulations requires enormous computing power. CST was instead used to calculate the resonant frequency and vane-tip voltage of each $\beta\lambda/2$ cell. The beginning and end of each cell is at the point of inflection, with purely transverse electric fields. Additionally, by symmetry, only one quadrant of the RFQ needs solving for the quadrupole mode. Thus Neumann boundaries ('magnetic boundaries' in CST) were implemented on the transverse planes and at either end of the cell to find the TE210 mode.

Fig. 5 shows how the resonant frequency and vane-tip voltage varies from cell to cell. There is a sharp 1.5MHz jump in local frequency at the end of the RFQ's gentle bunching section at 1.6m as the modulation depth rapidly increases. This causes a smooth field tilt along the whole RFQ, in agreement with (2). As the beam dynamics will not tolerate a ±40% variance relative to the desired 42.5kV, a flexible method to adjust the tilt was developed.

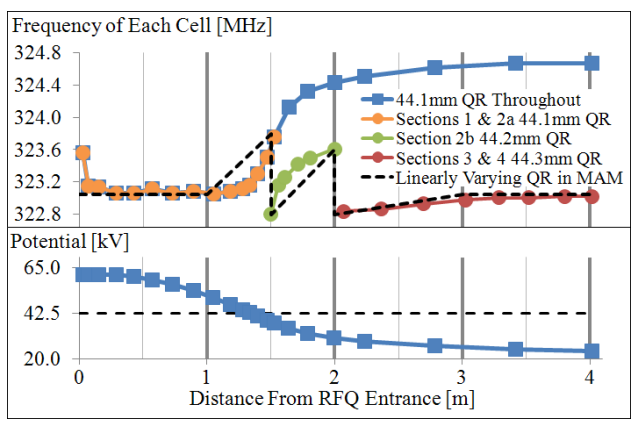

Figure 5: Resonant frequency and voltage of each cell. Squares: constant quadrant radius in every cell. Circles: optimised quadrant radius for each group of cells. Dashed line: modulation-less approximation model.

4m Modulation-less Approximation Model

To remove the frequency shift, the reduced capacitance caused by large modulations must be counteracted by an increase in inductance, by (3). This is achieved by moving the cavity walls away from the beam axis, increasing the total cavity volume; the same principle used by tuners.

The FETS RFQ is rather unique in its circular quadrant cross section, so the inductance can be tuned by varying the quadrant radius (QR). An eigenmode simulation of a 10mm-long slice of a 44.0mm radius RFQ quadrant with un-modulated vane tips was performed in ANSYS and CST and compared with a Superfish 2D result. All codes converged to the same frequency of 324.135MHz. It was found that the frequency linearly changes with QR. Using this fact, the frequency of groups of cells was corrected by altering the QR of each group. To ease machining of the RFQ quadrant walls, cells were grouped according to their position in the four 1m RFQ sections. The resulting shifted frequency of the cell groups is shown by coloured circles in Fig. 5. Unfortunately, the corresponding corrected voltage profile of the coupled system of all 308 cells could not be seen using this method.

Therefore, a simulation strategy was devised whereby the altered capacitance of the modulations was approximated by an altered inductance in a modulation-free RFQ; the two having equal effect on frequency, by (3). This simulation is hereafter referred to as the modulation-less approximation model (MAM). The QR in the MAM was linearly varied to reasonably approximate the modulation-induced frequency variation; this is shown by the dashed black line in Fig. 5.

In this manner, for example, a 43.9mm QR in the MAM has the same (elevated) frequency as a 44.1mm QR at the final modulation, cell 308. To shift the frequency of this cell down to the same as cell 1 requires a MAM QR of 44.1mm, or a modulated QR of 44.3mm. Using tapering QRs in the MAM allowed the modulation-induced field tilt to be easily simulated and fixed, as shown in Fig. 6.

In summary, adjusting the cavity inductance by varying the quadrant radius along the length of the RFQ has reduced the modulation-induced field tilt from ±40% to ±4%, which is much easier for the slug tuners to flatten.

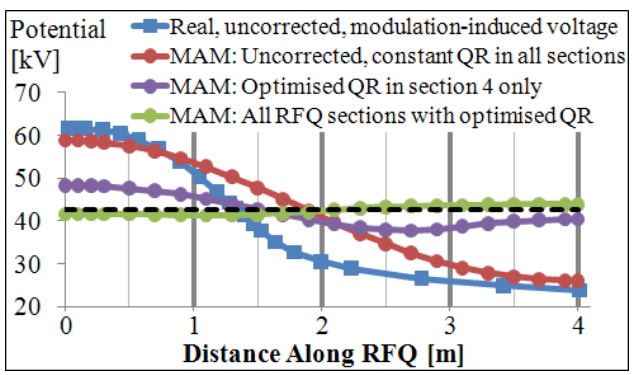

Figure 6: Varying the quadrant radius of each group of cells in stages using the modulation-less approximation model to achieve a flat field. Squares: individual cell voltages copied from Fig. 5 to compare with the MAM.

Field-Flattening Grooves

The real RFQ will be bolted together from major and minor vane pieces, which meet at the boundary of circular-shaped quadrants. Varying the quadrant radius would make the joining of these pieces difficult. Therefore, the cavity inductance will instead be varied by milling a series of grooves of different depths into the quadrants using a ball-ended cutter; demonstrated in Fig. 7. The field flattening grooves leave the bulk RFQ design unchanged and are easy to machine. Although non-adjustable, they will considerably ease the procedure needed to tune for a flat accelerating field.

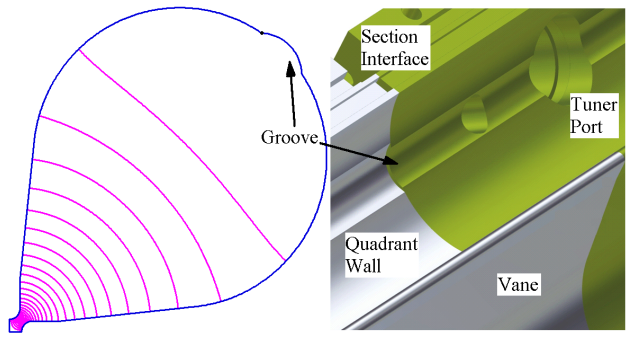

Figure 7: Superfish model (left) of an RFQ quadrant with groove cut into wall. CAD model (right) showing the join between two RFQ sections with different groove depths.

SUMMARY

The RF simulations performed of the FETS RFQ improve confidence that there will not be any unexpected problems arising during the tuning procedure. The radial matching section and modulations detrimentally affect field flatness, which would be difficult and costly to correct for. The frequency of the dipole mode can be widely modified by using end-wall fingers. The end region of the RFQ, which includes the radial matcher and vane cut-back, has been tuned to the correct frequency. Different depth grooves will be cut into the cavity walls to counteract the reducing capacitance of the modulations. As such, the RF performance of the FETS RFQ should meet the requirements to efficiently accelerate beam.

REFERENCES

[1] P. Savage *et al*, IPAC'10, MOPD056.
[2] A. Letchford *et al*, IPAC'10, MOPEC075.
[3] A. Letchford and A. Schempp, EPAC'98, THP11E.
[4] S. Jolly *et al*, IPAC'10, MOPEC076.
[5] M. Comunian *et al*, LINAC'08, MOP036.
[6] G. Romanov and A. Lunin, LINAC'08, MOP042.
[7] A. Ueno and Y. Kondo, LINAC'00, TUD02.
[8] O. Delferrière *et al*, EPAC'06, MOPCH105.
[9] S. Jolly *et al*, EPAC'08, THPP024.
[10] T. Wangler, *RF Linear Accelerators*, Wiley-VCH.